Marked Improvement in Photoinduced Cell Death by a New Tris-Heteroleptic Complex with Dual Action: Singlet Oxygen Sensitization and Ligand Dissociation.

8 AUTHORS, INCLUDING:

Christiane Pavani
Universidade Nove de Julho
16 PUBLICATIONS **141** CITATIONS

SEE PROFILE

Mauricio Baptista
University of São Paulo
155 PUBLICATIONS **2,411** CITATIONS

SEE PROFILE

Kim R Dunbar
Texas A&M University
442 PUBLICATIONS **13,341** CITATIONS

SEE PROFILE

Claudia Turro
The Ohio State University
143 PUBLICATIONS **3,651** CITATIONS

SEE PROFILE

J|A|C|S

JOURNAL OF THE AMERICAN CHEMICAL SOCIETY

Marked Improvement in Photoinduced Cell Death by a New Tris-heteroleptic Complex with Dual Action: Singlet Oxygen Sensitization and Ligand Dissociation

Bryan A. Albani,[§,†] Bruno Peña,[‡,†] Nicholas A. Leed,[§] Nataly A. B. G. de Paula,[#] Christiane Pavani,[#] Mauricio S. Baptista,[#] Kim R. Dunbar,*,[‡] and Claudia Turro*,[§]

[§]Department of Chemistry and Biochemistry, The Ohio State University, Columbus, Ohio 43210, United States

[‡]Department of Chemistry, Texas A&M University, College Station, Texas 77842, United States

[#]Department of Biochemistry, University of São Paulo, São Paulo 05508-070, Brazil

S *Supporting Information*

ABSTRACT: The new tris-heteroleptic complex $[Ru(bpy)(dppn)(CH_3CN)_2]^{2+}$ (**3**, bpy = 2,2′-bipyridine, dppn = benzo[i]dipyrido[3,2-a;2′,3′-c]phenazine) was synthesized and characterized in an effort to generate a molecule capable of both singlet oxygen ($^1O_2$) production and ligand exchange upon irradiation. Such dual reactivity has the potential to be useful for increasing the efficacy of photochemotherapy drugs by acting via two different mechanisms simultaneously. The photochemical properties and photoinduced cytotoxicity of **3** were compared to those of $[Ru(bpy)_2(dppn)]^{2+}$ (**1**) and $[Ru(bpy)_2(CH_3CN)_2]^{2+}$ (**2**), since **1** sensitizes the production of $^1O_2$ and **2** undergoes ligand exchange of the monodentate CH_3CN ligands with solvent when irradiated. The quantum yield of $^1O_2$ production was measured to be 0.72(2) for **3** in methanol, which is slightly lower than that of **1**, $\Phi = 0.88(2)$, in the same solvent ($\lambda_{irr} = 460$ nm). Complex **3** also undergoes photoinduced ligand exchange when irradiated in H_2O ($\lambda_{irr} = 400$ nm), but with a low quantum efficiency (<1%). These results are explained by the low-lying ligand-centered $^3\pi\pi^*$ excited state of **3** localized on the dppn ligand, thus decreasing the relative population of the higher energy ^3dd state; the latter is associated with ligand dissociation. Cytotoxicity data with HeLa cells reveal that complex **3** exhibits a greater photocytotoxicity index, 1110, than does either **1** and **2**, indicating that the dual-action complex is more photoactive toward cells in spite of its low ligand exchange quantum yield.
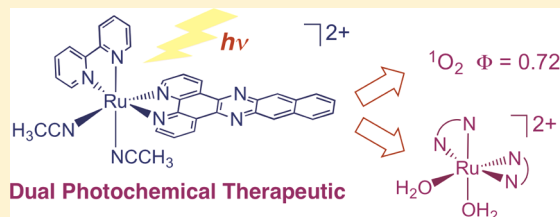
INTRODUCTION

Due to the drawbacks of many conventional chemotherapeutic treatments, including poor selectivity for tumor tissue and drug resistance, a wide variety of new drugs have been developed with varying levels of success.[1−7] Many of these treatments rely on either direct damage to DNA or disruption of the redox homeostasis of the tumor cell.[1−9] One approach to circumvent the drawbacks of the common current anticancer therapies is to develop new strategies whereby an external source can be used to activate the drug. The use of light for drug activation, photochemotherapy (PCT), is invoked to induce cell death only upon irradiation, which can be operative via a number of mechanisms, including redox reactions, damage to biological targets, or the production of a reactive species. An important consideration for a successful PCT agent is for the molecule to be nontoxic in the dark, such that it is only activated through the absorption of light. PCT provides low systemic toxicity, low levels of invasiveness, and increased selectivity, and in some cases it is superior to conventional cancer therapies.[10−13]

Research in the area of PCT that has demonstrated promising results to date includes molecules that photosensitize the production of singlet oxygen compounds ($^1O_2$, commonly known as photodynamic therapy agents) that release drugs when irradiated, and transition metal complexes that covalently bind to DNA when photolyzed.[14−19] Although compounds approved for PCT and those currently undergoing clinical trials are almost all organic molecules that produce $^1O_2$ upon irradiation,[14] inorganic complexes that possess ligands with extended π-systems and long excited-state lifetimes have been shown to sensitize $^1O_2$ with significantly greater efficiency than those currently in use;[20−23] these species include $[Ru(bpy)_2(dppn)]^{2+}$ (**1**; bpy = 2,2′-bipyridine, dppn = benzo[i]dipyrido-[3,2-a;2′,3′-c]phenazine), whose structure is schematically depicted in Figure 1.[24] Upon irradiation with visible light, complex **1** produces $^1O_2$ with quantum yield $\Phi = 0.88$ from a long-lived dppn $^3\pi\pi^*$ excited state and efficiently photocleaves DNA, but it is not reactive toward the DNA duplexes in the dark. Moreover, complexes with extended π-systems have been shown to exhibit strong intercalative binding to DNA.[25−27]

In addition to intercalation, inorganic complexes are also able to bind covalently to DNA by attachment of the metal center. Such metal nucleobase coordination represents a key feature of the mechanism of action of cisplatin, one of the current leading
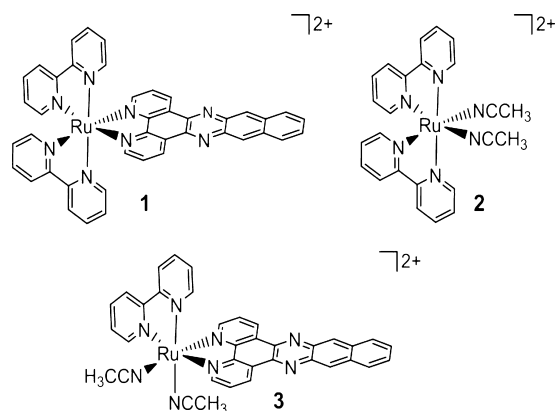
Figure 1. Schematic representation of the molecular structures of **1**–**3**.

anticancer drugs.[8,9] Transition metal complexes with photolabile ligands are able to covalently bind to DNA in a manner similar to that of cisplatin, but only upon irradiation with visible light. The requirement of the use of photons for their activation results in increased spatiotemporal selectivity toward tumor tissue relative to traditional drugs.[14,15] Moreover, transition metal complexes that are activated by light have been shown to be less toxic in the dark and to exhibit a greater increase in cytotoxicity upon irradiation than the organic compounds currently approved for PCT.[16,28−31] One such complex, *cis*-[Ru(bpy)$_2$(CH$_3$CN)$_2$]$^{2+}$ (**2**, Figure 1), exhibits a relatively high quantum yield for ligand exchange with water to yield [Ru(bpy)$_2$(H$_2$O)$_2$]$^{2+}$ (Φ_{400} = 0.21), a value that is significantly greater than those found with related Ru(II) complexes.[16,32,33]

Ultrafast experiments previously showed that **2** violates Kasha's rule through simultaneous population of both its short-lived ^{3}MLCT state, τ = 51 ps, and the ^{3}LF (ligand-field) states; the latter results in fast ligand exchange in water.[28] The high quantum yields for exchange of the nitrile ligands in **2** and its ability to simultaneously populate two different upon excitation through ultrafast intersystem crossing (ISC), together with the efficient sensitization of ^{1}O$_2$ by **1**, provide a platform for the possible combination of the two features to generate a new PCT agent that may simultaneously act via two different mechanisms, the production of ^{1}O$_2$ and covalent binding to DNA upon irradiation, while remaining inactive in the dark. To this end, the tris-heteroleptic complex [Ru(bpy)(dppn)-(CH$_3$CN)$_2$]$^{2+}$ (**3**) was synthesized, and its photophysical properties and phototoxicity were compared to those of **1** and **2** (Figure 1).

■ EXPERIMENTAL SECTION

Materials. Standard Schlenk-line techniques (N$_2$ atmosphere) were used to maintain anaerobic conditions during the preparation of the compounds. The solvents used were of reagent grade quality. Normal butanol (*n*-BuOH, Mallinckrodt), water (ChromAR, Mallinckrodt), and acetonitrile (EMD Chemicals) were used as received. The reagents RuCl$_3$·3H$_2$O (Pressure Chemicals), 2,2′-bipyridine (Alfa Aesar), potassium ferrioxalate (Strem Chemicals), 1,3-diphenyl-isobenzofuran (DPBF, Sigma-Aldrich), and NH$_4$PF$_6$ (Sigma-Aldrich) were purchased and used without further purification. The compounds [Ru(bpy)$_2$(dppn)][PF$_6$]$_2$ (**1**),[34] *cis*-[Ru(bpy)$_2$(NCCH$_3$)$_2$][PF$_6$]$_2$ (**2**),[24] [(η^6-C$_6$H$_6$)RuCl(bpy)][Cl],[35] Ru(bpy)(DMSO)$_2$Cl$_2$,[36] and the dppn ligand[37] were prepared according to literature procedures.

[Ru(bpy)(dppn)(CH$_3$CN)$_2$][PF$_6$]$_2$ (3). *Method 1.* An orange suspension of [(η^6-C$_6$H$_6$)RuCl(bpy)][Cl] (201 mg, 0.49 mmol) and dppn (165 mg, 0.50 mmol) in *n*-BuOH (15 mL) was refluxed for 14 h under reduced light conditions. The solvent was then removed under reduced pressure to give a dark purple-red solid residue which was dissolved in CH$_2$Cl$_2$ (400 mL) to give a dark red solution. After filtration, the solution was washed with water several times, and the resulting dark purple organic layer was dried with anhydrous MgSO$_4$ and reduced to ca. 10 mL. A dark purple solid (*cis*-RuCl$_2$(bpy)(dppn)) was obtained upon precipitation with diethyl ether (25 mL). This intermediate (28 mg, 42.5 μmol) was suspended in 3 mL of MeCN/H$_2$O (2:1), and the suspension was heated at 100 °C for 3 h under reduced light conditions. The resulting dark orange solution was filtered while hot through a plug of glass wool, and NH$_4$PF$_6$ (110 mg) dissolved in 1 mL of H$_2$O was added dropwise to the filtrate. The resulting orange precipitate was collected by filtration, dissolved in 1.5 mL of hot MeCN, and precipitated by slow addition of hot H$_2$O. After the mixture was stored in a freezer for 4 h, the orange precipitate was collected by filtration and washed with H$_2$O (3 × 3 mL) and diethyl ether (15 mL). Yield: 24 mg (5%). ^{1}H NMR (500 MHz, (CD$_3$)$_2$CO, Supporting Information, Figure S1): δ 10.03 (dd, 1H, ^3J = 5.5 Hz, ^4J = 1.0 Hz, H-*l*), 9.91 (dd, 1H, ^3J = 8.0 Hz, ^4J = 1.0 Hz, H-*j*), 9.73 (d, 1H, ^3J = 5.5 Hz, H-1), 9.60 (dd, 1H, ^3J = 8.0 Hz, ^4J = 1.5 Hz, H-*c*), 9.19 (s, 1H, H-*d* or H-*i*), 9.13 (s, 1H, H-*i* or H-*d*), 8.88 (d, 1H, ^3J = 8.0 Hz, H-4), 8.71 (d, 1H, ^3J = 8.0 Hz, H-5), 8.50−8.45 (m, 2H, H-3, H-*k*), 8.41 (m, 2H, H-*f*, H-*g*), 8.33 (dd, 1H, ^3J = 5.5 Hz, ^4J = 1.0 Hz, H-*a*), 8.10−8.03 (m, 2H, H-2, H-6), 8.01 (d, 1H, ^3J = 5.5 Hz, H-8), 7.92 (dd, 1H, ^3J = 8.0 Hz, 5.5 Hz, H-*b*), 7.78 (m, 2H, H-*e*, H-*h*), 7.32 (ddd, 1H, ^3J = 7.5 Hz, 5.5 Hz, ^4J = 1.0 Hz, H-7), 2.58 (s, 3H, NCCH$_3$), 2.41 (s, 3H, NCCH$_3$). Anal. Calcd for C$_{36}$H$_{26}$F$_{12}$N$_8$P$_2$Ru·0.9 H$_2$O: C, 44.22; H, 2.87; N, 11.46. Found: C, 44.25; H, 2.92; N, 11.39.

Method 2. Ru(bpy)(DMSO)$_2$Cl$_2$ (51 mg, 0.11 mmol) and 1 equiv of the dppn ligand (35 mg, 0.11 mmol) were suspended in 8 mL of DMF and heated to reflux for 6 h. The reaction mixture was cooled to room temperature, and the solvent was removed by rotary evaporation, resulting in a dark black solid. The solid was suspended in 50 mL of CH$_2$Cl$_2$ and collected by vacuum filtration. The dark solid (*cis*-RuCl$_2$(bpy)(dppn)) was subsequently washed with a copious amount of H$_2$O and then 30 mL of diethyl ether. This intermediate (10 mg, 0.015 mmol) was suspended in a 12 mL CH$_3$CN:H$_2$O (1:1) solvent mixture and heated to reflux in the dark for 16 h. While hot, a saturated aqueous solution of NH$_4$PF$_6$ (5 mL) was added to the resulting orange reaction mixture. Upon cooling, an orange precipitate formed which was collected by vacuum filtration. The precipitate was washed with 20 mL of H$_2$O and 20 mL of diethyl ether. Product characterization results matched those of Method 1. Yield 4.4 mg (4%).

Instrumentation. ^{1}H NMR spectra were recorded on a Varian 500 MHz spectrometer. Steady-state absorption spectra were recorded on a Hewlett-Packard 8453 diode array spectrometer, and emission data for ^{1}O$_2$ experiments were collected on a Horiba Fluoromax-4 spectrometer. Electrochemical measurements were carried out by using an HCH electrochemical analyzer (model CH 1620A). Nanosecond transient absorption was carried out using a home-built instrument previously reported,[38] using a frequency-tripled (355 nm) Spectra Physics GCR-150 Nd:YAG laser (fwhm ∼8 ns) as the excitation source. Femtosecond transient absorption experiments were carried out using laser and detection systems that were previously described.[39] The sample was excited at 300 nm (1.5 mW at the sample) by the output of an optical parametric amplifier with a sum frequency generator and ultraviolet−visible harmonics attachment. Upon irradiation, samples were kept in motion by use of a Harrick Scientific flow cell equipped with 1 mm CaF$_2$ windows (1 mm path length). A total volume of ∼10 mL was required for the flow cell to operate correctly. The polarization angle between the pump and probe beams was 54.7° to avoid rotational diffusion effects. Measurement at each time delay was repeated four times, and the spectra were corrected for the chirp in the white light probe continuum.[40] Ligand-exchange quantum yields and photolysis experiments were performed using a 150 W Xe short arc lamp (USHIO) in a Miliarc lamp housing unit (PTI) powered by an LPS-220 power supply (PTI) equipped with an LPS-221 igniter (PTI). Bandpass filters (Thorlabs, fwhm ∼10 nm) and 3 mm thick long-pass filters (CVI Melles Griot) were used to attain desired excitation wavelengths.

187   **Methods.** ^{1}H NMR spectral studies were performed in acetone-d_6
188 ((CD$_3$)$_2$CO), and all chemical shifts (δ) are reported in parts per
189 million (ppm) and internally referenced to the residual acetone peak
190 (2.05 ppm). Emission experiments were measured using a 1 × 1 cm^2
191 quartz cuvette. Cyclic voltammetric measurements were performed in
192 CH$_3$CN (distilled from 3 Å molecular sieves) with 0.1 M tetra-n-
193 butylammonium hexafluorophosphate, [^{n}Bu$_4$N][PF$_6$], as the support-
194 ing electrolyte. The working electrode was a BAS Pt disk electrode, the
195 reference electrode was Ag/AgCl (3 M KCl), and the auxiliary
196 electrode was a Pt wire. The ferrocene/ferrocenium couple occurs at
197 $E_{1/2}$ = +0.44 V vs Ag/AgCl under the same experimental conditions.
198 Elemental analyses were performed by Atlantic Microlab Inc.
199 (Norcross, GA). The ^{1}O$_2$ quantum yields for complex **3** were
200 measured using [Ru(bpy)$_3$]$^{2+}$ as the standard (Φ = 0.81 in CH$_3$OH)
201 and DPBF as a trapping agent, with 460 nm irradiation.[41] The
202 experiment was performed by absorption matching **3** and the standard
203 at the irradiation wavelength (0.01 at 460 nm). The complexes were
204 irradiated at regular time intervals in the presence of DPBF (1.0 μM),
205 and the decrease in emission of DPBF was monitored as a function of
206 time (λ_{ex} = 405 nm, λ_{em} = 479 nm). The DPBF emission intensity vs
207 irradiation time was plotted, and the slopes of the standard and **3** were
208 compared to give the ^{1}O$_2$ quantum yield. Data points were collected
209 for each complex until the slopes became nonlinear. The quantum
210 yields for photoinduced ligand exchange in **2** and **3** were measured at
211 an irradiation wavelength of 400 nm in H$_2$O using potassium
212 ferrioxalate as the actinometer following an established procedure.[42]
213   The IC$_{50}$ values were determined using the human cervical
214 adenocarcinoma cell line (HeLa cells, ATCC CCL-2) cultured in
215 Dulbecco's modified eagle medium (DMEM) supplemented with 10%
216 fetal bovine serum (FBS) and 1% penicillin/streptomycin at 37 °C in a
217 humid incubator with 5% CO$_2$. Cells were seeded in 48-well plates
218 (1.5 × 10^4 cells/well) and, after attachment, were exposed to the
219 complexes **1**–**3** in DMEM/1% FCS during 24 h from 0 to 750 μM.
220 Each well was then washed with phosphate-buffered saline (PBS 1
221 mM, pH 7.2), and fresh PBS was added to the wells. One plate was
222 then irradiated for 20 min (LED system 466 ± 20 nm; 6.50 mW/cm^2),
223 while the other was kept in the dark during that time. After irradiation,
224 PBS was replaced with DMEM/1% FCS, and the plates were kept in
225 the incubator for an additional 48 h, at which time the MTT assay was
226 conducted using methods described previously.[43]
227   Cellular uptake studies were conducted using 12-well plates (1 ×
228 10^5 HeLa cells per well). The plates were maintained in DMEM
229 supplemented with 10% FCS and 1% penicillin/streptomycin in an
230 incubator at 37 °C in a humid atmosphere with 5% CO$_2$ for 18–24 h.
231 After washing with PBS, each well was filled with a 200 μM solution of
232 complex in DMEM/1% FCS and incubated for 24 h in the dark. After
233 that time, 500 μL of the supernatant was removed from each well for
234 quantification, to which 500 μL of 50 mM SDS was added. The spare
235 supernatant from each well was removed and discarded. The
236 remaining cells were washed with PBS, followed by the addition of
237 500 μL of a 25 mM SDS solution to promote lysis of the cellular
238 membrane. These solutions were used to quantify the ruthenium
239 complex taken up by the cells, determining the absorbance at the
240 wavelength of maximum absorption (Shimadzu UV-2401PC spectro-
241 photometer) using the corresponding molar extinction coefficient in
242 the lysed solutions, A_{lysed}, relative to that of the supernatant, $A_{supernatant}$
243 via the equation (% uptake) = [(A_{lysed}/2)/(2$A_{supernatant}$ + A_{lysed}/2)] ×
244 100.[43]

■ RESULTS AND DISCUSSION
245

246   **Electronic Absorption Spectroscopy and Electro-**
247 **chemistry.** The steady-state electronic absorption spectra of
248 **1**–**3** in CH$_3$CN are provided in Figure 2a. The absorption
249 spectrum of **1** exhibits dppn-based $^1\pi\pi^*$ transitions with
250 maxima at 387 nm (9900 M^{-1} cm^{-1}) and 411 nm (13 400 M^{-1}
251 cm^{-1}) that are similar to those of the free dppn ligand in CHCl$_3$
252 observed at 390 nm (9400 M^{-1} cm^{-1}) and 414 nm (12 500
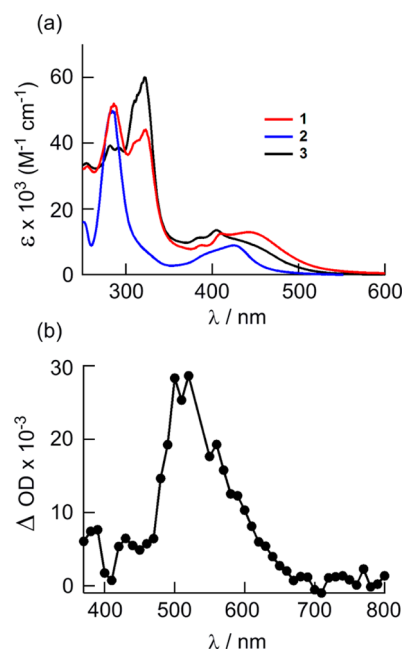253 M^{-1} cm^{-1}). These ligand-centered transitions are slightly blue-

Figure 2. (a) Electronic absorption spectra of complexes **1**–**3** in
CH$_3$CN. (b) Transient absorption spectrum of **3** in CH$_3$CN collected
0.2 μs after the excitation pulse (λ_{exc} = 355 nm, fwhm ∼8 ns).

shifted and more intense in **3**, with maxima at 382 nm (11 100 254
M^{-1} cm^{-1}) and 405 nm (13 500 M^{-1} cm^{-1}). The typical 255
^{1}MLCT bands arising from Ru(dπ)→L(π^*) transitions are 256
prominent in **1** and **3**, centered at 444 nm (13 500 M^{-1} cm^{-1}) 257
and 430 nm (11 000 M^{-1} cm^{-1}), respectively, and blue-shifted 258
with maximum at 425 nm (8900 M^{-1} cm^{-1}) in **2**. 259

Cyclic voltammetric measurements reveal that **2** and **3** 260
exhibit a reversible metal-based oxidation event at 261
$E_{1/2}$([Ru]$^{3+/2+}$) = +1.74 and +1.69 V vs NHE, respectively, 262
both of which are more positive than the respective redox 263
events in [Ru(bpy)$_3$]$^{2+}$, +1.54 V vs NHE, and **1**, +1.58 V vs 264
NHE (Supporting Information, Figures S2 and S3, respec- 265
tively).[20] This cathodic shift is ascribed to the greater π- 266
backbonding afforded by the acetonitrile ligands in **2** and **3**. 267
Both complexes exhibit quasi-reversible redox events at 268
negative potentials which involve reduction of the polypyridyl 269
ligands. Compound **3** shows a characteristic dppn ligand-based 270
reduction at $E_{1/2}$([Ru]$^{2+/+}$) = −0.46 V vs NHE, which occurs at 271
less negative potentials than the bpy reduction in **1**, 272
$E_{1/2}$([Ru]$^{2+/+}$) = −1.14 V vs NHE, as has been noted in the 273
literature for other Ru-dppn compounds.[20,44] 274

Excited-State Properties. Nanosecond transient absorp- 275
tion spectra (λ_{exc} = 355 nm, fwhm ∼8 ns) measured in 276
deaerated CH$_3$CN reveal a strong absorption band at ∼540 nm 277
for **3** with τ = 20 μs, shown in Figure 2b. Similar features are 278
observed for **1** under the same experimental conditions and the 279
free dppn ligand in CHCl$_3$, with τ = 33 μs and τ = 18 μs, 280
respectively, and are assigned as the $^3\pi\pi^*$ excited state on the 281
dppn ligand.[20] Therefore, the lowest energy excited state in **3** is 282
the $^3\pi\pi^*$ state centered on the dppn ligand. In contrast, **2** 283
exhibits a very short ^{3}MLCT lifetime of 51 ps at room 284
temperature in CH$_3$CN owing to the competing ligand 285
dissociation process and thermal depopulation of the ^{3}MLCT 286
state through the ^{3}LF state(s), expected to lie at a slightly 287
higher energy.[24] The different spectral profile and short lifetime 288

of the ^{3}MLCT state of **2** further support that the excited state of **3** is the low-lying dppn $^3\pi\pi^*$ state.[24]

As previously reported, the ^{3}MLCT states of **1** and **2** are populated within the ~300 fs laser pulse (310 and 385 nm), as expected from the known fast ISC rates typical of Ru(II) complexes, and are vibrationally cooled within ~1 ps.[20] A point of interest is that the population of both the ^{3}MLCT and dppn-centered $^3\pi\pi^*$ states is observed in **1** and **3** within the excitation with an ultrafast laser pulse (~300 fs, 300−355 nm). Previously reported ultrafast transient absorption spectra of **1** in CH$_3$CN are consistent with the formation of a vibrationally cooled dppn $^3\pi\pi^*$ state with $\tau \approx 2$ ps.[20] In that case, the population of ^{3}MLCT state is observed at $t < 5$ ps but is relatively small, and it is not clear whether the ^{3}MLCT state decays back to the ground state or to the dppn $^3\pi\pi^*$ state. Figure 3a shows the
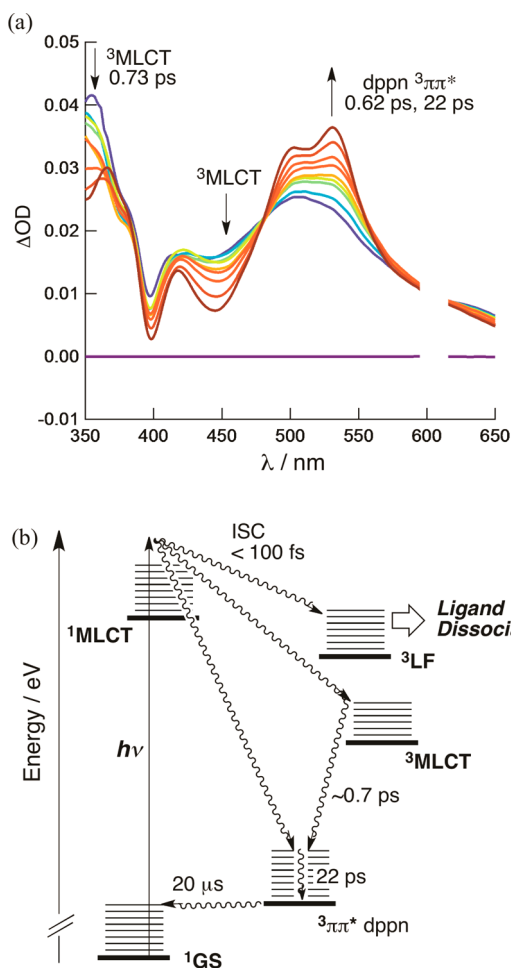

Figure 3. (a) Transient absorption spectra of **3** in CH$_3$CN collected at 0.1, 0.5, 1, 2, 3, 5, 10, 20, and 40 ps following the excitation pulse (λ_{exc} = 300 nm, fwhm ~300 fs). (b) Jablonski diagram for the excited-state dynamics of **3** in CH$_3$CN.

The ^{3}MLCT signal at 365 nm can be fitted to a monoexponential decay with $\tau = 720$ fs, while the rise time of the $^3\pi\pi^*$ peak at 540 nm follows a biexponential growth, with $\tau_1 = 630$ fs and $\tau_2 = 22$ ps (Figure 3). Given the similarity of the fast time constant, the growth of the signal at 540 nm at early times is believed to arise from internal conversion (IC) from the ^{3}MLCT to the $^3\pi\pi^*$ state. The sharpening of the 540 nm signal occurs with a time constant of 22 ps, attributed to vibrational cooling. The excited-state dynamics of **3** in CH$_3$CN are schematically depicted in the Jablonski diagram shown in Figure 3b. Ligand dissociation likely proceeds through direct population of the ^{3}LF (ligand field) states from the Franck− Condon state (Figure 3b) but is not observed under the present experimental conditions because of the low quantum yield for this process.

The difference in the relative initial populations of the ^{3}MLCT and $^3\pi\pi^*$ states in **1** and **3** can be explained by higher energy ^{1}MLCT and ^{3}MLCT states in **3** as compared to **1**, while the $^3\pi\pi^*$ state in both complexes is expected to remain constant. The greater ^{1}MLCT−$^3\pi\pi^*$ energy gap in **3** results in a slower ISC ^{1}MLCT→$^3\pi\pi^*$ rate than in **1**, while the ^{1}MLCT−^{3}MLCT rate constant is expected to be similar in the two compounds. The slower ^{1}MLCT→$^3\pi\pi^*$ rate results in a greater relative population of the ^{3}MLCT vs $^3\pi\pi^*$ state in **3** versus **1**.

Photosensitization of ^{1}O$_2$ and Photoinduced Ligand Exchange. The changes in the electronic absorption spectrum of **3** in H$_2$O as a function of irradiation time are shown in Figure 4. A red shift is observed in the spectrum at early times,
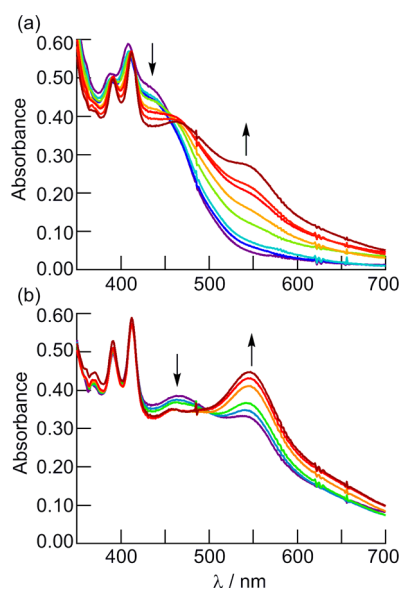

Figure 4. Changes in the electronic absorption spectrum of **3** (20 μM) in H$_2$O as a function of irradiation time, collected at (a) 0, 1, 2, 5, 10, 15, 20, and 30 min and (b) 40, 50, 60, 100, 120, and 210 min (λ_{irr} = 400 nm).

presence of a significantly greater relative population of the ^{3}MLCT state in **3** as compared to **1** (λ_{exc} = 300 nm, fwhm ~300 fs), evident at 350−365 nm and in the 430−470 nm range. The sharp ground-state absorption features of the $^1\pi\pi^*$ transitions of the dppn at ~400 nm are superimposed as bleach signals on the positive transient absorption spectrum, which resemble the spectra reported for **1** (Figure 3a).

with the appearance of new features with maxima at ~470 and ~540 nm (Figure 4). Over a longer photolysis period, the ~470 nm peak begins to decrease in intensity, with concomitant growth of a band with a maximum at 547 nm. Overall, a final shift in the MLCT absorption maximum from 430 to 547 nm is observed; the latter is consistent with the formation of the product [Ru(bpy)(dppn)(H$_2$O)$_2$]$^{2+}$. This shift in energy (4737

Table 1. Toxicity Data in the Dark and upon Irradiation for 1−3

complex	RA[a]	$IC_{50}^{dark}/\mu M$[b]	$IC_{50}^{irr}/\mu M$[b]	PI[c]	PI_{cor}[d]
1	1	110 ± 28	0.39 ± 0.06	282 ± 69	282 ± 69
2	0.17	244 ± 23	223 ± 94	1.1 ± 0.4	6.4 ± 2.3
3	0.64	334 ± 74	0.47 ± 0.02	711 ± 132	1110 ± 206

[a]Molar absorptivity relative to that of 1 at the irradiation wavelength for phototoxicity studies (466 nm). [b]IC$_{50}$ represents the concentration required to attain 50% cell death; IC$_{50}^{irr}$ value determined by irradiating the cell culture with a 466 ± 20 nm LED for 20 min and then incubating for 48 h; errors determined from two or three experimental trials. [c]Phototoxicity index: PI = IC$_{50}^{dark}$/IC$_{50}^{irr}$. [d]Corrected PI value: PI$_{cor}$ = PI/RA.

cm^{-1}) upon forming the bis-aqua species is similar to that in 2 (3121 cm^{-1}) and other related Ru(II) complexes, in which two CH$_3$CN ligands are replaced by two water molecules.[24,45] No changes in the electronic absorption spectrum of 3 are observed when the complex is stored in the dark in water under similar experimental conditions (Supporting Information, Figures S5 and S6).

The quantum yield for the first ligand exchange, Φ_{ex}, for 3 in H$_2$O to form cis-[Ru(bpy)(dppn)(CH$_3$CN)(H$_2$O)]$^{2+}$ was measured to be 0.002(3) with λ_{irr} = 400 nm, a value that is 2 orders of magnitude lower than that measured for 2 to form [Ru(bpy)$_2$(CH$_3$CN)(H$_2$O)]$^{2+}$, Φ_{ex} = 0.21, under similar irradiation conditions.[16c] Population of the dissociative ^{3}LF state(s) with Ru−CH$_3$CN(σ^* character), either directly from the ^{1}MLCT state or due to thermal population from the ^{3}MLCT state, is required for ligand dissociation to take place (Figure 3b).[46−49] The low-lying $^3\pi\pi^*$ state in 3, which is not present in 2, results in fast ^{3}MLCT−^{3}LF IC ($\tau \approx 0.7$ ps), such that thermal population of the higher-lying ^{3}LF state from the ^{3}MLCT does not favorably compete with IC. In addition, ISC from the ^{1}MLCT state in 3 is partitioned between the three available triplet states, ^{3}LF, ^{3}MLCT, and $^3\pi\pi^*$ (Figure 3b), instead of only two states in 2, ^{3}LF and ^{3}MLCT. The presence of an additional low-lying $^3\pi\pi^*$ state reduces the population of the ^{3}LF state and, therefore, the quantum yield of ligand dissociation.

The long lifetime of the $^3\pi\pi^*$ excited state of 3 is expected to result in the sensitization of ^{1}O$_2$. The quantum yield for the generation of ^{1}O$_2$, Φ_Δ, by 3 was measured to be 0.72(2) (λ_{irr} = 460 nm) using 1,3-diphenylisobenzofuran (DPBF) as a trapping agent and [Ru(bpy)$_3$]$^{2+}$ as a standard (Φ_Δ = 0.81) in methanol (Supporting Information, Figure S4). This value is slightly lower than that previously reported for 1, Φ_Δ = 0.88(2) in the same solvent,[20] which may be due to the competing photoinduced ligand-exchange process.

Cytotoxicity. Table 1 lists cytotoxicity and phototoxicity data for 1−3 toward HeLa cancer cells, the relative molar absorptivity (RA) of each complex at the irradiation wavelength (466 nm), and the phototoxcity index (PI). It is evident from Table 1 that 3 is the least toxic complex when incubated in the dark for 48 h, with half-maximal inhibitory concentration, IC$_{50}^{dark}$, of 334 μM, followed by 2 (IC$_{50}^{dark}$ = 244 μM) and then 1 (IC$_{50}^{dark}$ = 110 μM). It should be noted that the phototoxicity enhancement of 2 toward HeLa cells under the present experimental conditions is modest (Table 1). A similar result was published recently using the PC3 cell line for the same complex.[50] In contrast, both 1 and 3 exhibit enhanced cytotoxicities upon irradiation with visible light (466 ± 20 nm), followed by incubation for 48 h in the dark, resulting in IC$_{50}^{irr}$ values of 390 and 470 nM, respectively. Although the photocytotoxicity of 3 is slightly lower than that of 1, the important factor in PCT is the relative toxicity when the complex is kept in the dark versus when it is irradiated, given by

PI = IC$_{50}^{dark}$/IC$_{50}^{irr}$. The PI value for 3 is 2.5-fold greater than that for 1 and represents the effective PCT activity of the complex.[51] The PI values for complexes 1 and 3 are 282 and 711, respectively, but 1 exhibits a greater absorption of the excitation wavelength, which is reported as the RA value in Table 1 (RA = relative molar extinction coefficient at 466 nm). It should be noted that the percent cellular uptake values of 1 and 3 were measured to be 5 ± 2% and 6 ± 2%, respectively, while that for 1 was 0.76 ± 0.03%. Given the similarity in hydrophobicity, overall charge, size, shape, and molecular structures of 1 and 3, the fact that their cellular uptake is nearly identical is expected and does not account for the difference in PI values measured for the complexes. The PI values corrected for difference in absorption at 466 nm, PI$_{cor}$, result in even greater phototoxicity of 3 relative to that of 1. This result is unexpected, since 1 is able to generate ^{1}O$_2$ in greater yields than 3, but complex 3 may be able to induce DNA cross-links, or it may bind to proteins or other biomolecules in the cell following photo-induced ligand exchange. This additional mode of action to ^{1}O$_2$ production may result in the enhanced phototoxicity of 3, with PI$_{cor}$ = 1110 ± 206.

CONCLUSIONS

In order to circumvent the drawbacks of current chemo-therapeutic treatments and improve upon current PCT agents, complex 3 was synthesized and characterized to function as a multimodal PCT complex capable of producing ^{1}O$_2$ and to undergo ligand exchange to potentially covalently bind DNA and other biomolecules upon irradiation. The photophysical properties of the new complex were compared to those of 1 and 2, which have been established to undergo efficient ^{1}O$_2$ production and ligand exchange when irradiated, respectively. Under analogous conditions, complex 3 produces ^{1}O$_2$ slightly less efficiently than 1, and photoinduced ligand exchange occurs in 3 to a much lesser extent than in 2. It appears, however, that 3 may be a more useful PCT agent since its corrected phototoxicty index, PI$_{cor}$, is nearly 3 times greater than that of 1. Future work includes designing complexes that improve upon the dual efficiency of ^{1}O$_2$ production and ligand exchange, as well as an investigation aimed at gaining further understanding of the mechanism of cell death.

ASSOCIATED CONTENT

S Supporting Information

^{1}H NMR data, cyclic voltammetry, singlet oxygen quantum yield data, complete photolysis data, and dark stability. This material is available free of charge via the Internet at http://pubs.acs.org.

AUTHOR INFORMATION

Corresponding Authors
dunbar@mail.chem.tamu.edu
turro.1@osu.edu

Author Contributions

†B.A.A. and B.P. contributed equally to this work.

Notes

The authors declare no competing financial interest.

■ REFERENCES

(1) Boulikas, T.; Vougiouka, M. Oncol. Rep. 2003, 10, 1663–1682.

(2) Go, R. S.; Adjei, A. A. J. Clin. Oncol. 1999, 17, 409–422.

(3) Nussbaumer, S.; Bonnabry, P.; Veuthey, J.; Fleury-Souverain, S. Talanta 2011, 85, 2265–2289.

(4) Fuertes, M. A.; Alonso, C.; Perez, J. M. Chem. Rev. 2003, 103, 645.

(5) Berner-Price, S. J.; Appleton, T. G. In Platinum-Based Drugs in Cancer Therapy; Kelland, L. R., Farrell, N., Eds.; Humana Press: Totowa, NJ, 2000; pp 3–31.

(6) Bergamo, A.; Gaiddon, C.; Schellens, J. H. M.; Beijnen, J. H.; Sava, G. J. Inorg. Biochem. 2012, 106, 90–99.

(7) Habtemariam, A.; Melchart, M.; Fernandez, R; Parsons, S.; Oswald, I. D. H.; Parkin, A.; Fabbiani, F. P. A.; Davidson, J. E.; Dawson, A.; Aird, R. E.; Jodrell, D. I.; Sadler, P. J. J. Med. Chem. 2006, 49, 6858–6868.

(8) Jamieson, E. R.; Lippard, S. J. Chem. Rev. 1999, 99, 2467–2498.

(9) Lovejoy, K. S.; Lippard, S. J. Dalton Trans. 2009, 48, 10651.

(10) Nyst, H. J.; Tan, I. B.; Stewart, F. A.; Balm, A. J. M. Photodiag. Photodyn. Ther. 2009, 6, 3–11.

(11) Allison, R. R.; Sibata, C. H. Photodiag. Photodyn. Ther. 2010, 7, 61–75.

(12) O'Connor, A. E.; Gallagher, W. M.; Byrne, A. T. Photochem. Photobiol. 2009, 85, 1053–1074.

(13) Zuluaga, M.-F.; Lange, N. Curr. Med. Chem. 2008, 15, 1655–1673.

(14) Dolmans, D. E.; Fukumura, D.; Jain, R. K. Nat. Rev. Cancer 2003, 3, 380–387.

(15) Moses, B.; You, Y. Med. Chem. 2013, 3, 192–198.

(16) (a) Garner, R. N.; Gallucci, J. C.; Dunbar, K. R.; Turro, C. Inorg. Chem. 2011, 50, 9213–9215. (b) Respondek, T.; Garner, R. N.; Herroon, M. K.; Podgorski, I.; Turro, C.; Kodanko, J. J. J. Am. Chem. Soc. 2011, 133, 17164–17167. (c) Singh, T. N.; Turro, C. Inorg. Chem. 2004, 43, 7260–7262. (d) Sgambellone, M. A.; David, A.; Garner, R. N.; Dunbar, K. R.; Turro, C. J. Am. Chem. Soc. 2013, 135, 11274–11282.

(17) Higgins, S. L. H.; Tucker, A. J.; Winkel, B. S. J.; Brewer, K. J. Chem. Commun. 2012, 48, 67–69.

(18) Lincoln, R.; Kohler, L.; Monro, S.; Yin, H.; Stephenson, M.; Zong, R.; Chouai, A.; Dorsey, C.; Hennigar, R.; Thummel, R. P.; Mcfarland, S. A. J. Am. Chem. Soc. 2013, 135, 17161–17175.

(19) Frasconi, M.; Liu, Z.; Lei, J.; Wu, Y.; Strekalova, E.; Malin, D.; Ambrogio, M. W.; Chen, X.; Botros, Y. Y.; Cryns, V. L.; Sauvage, J.; Stoddart, J. F. J. Am. Chem. Soc. 2013, 135, 11603–11613.

(20) DeRosa, M. C.; Crutchley, R. J. Coord. Chem. Rev. 2002, 233–244, 351–357.

(21) Ashen-Garry, D.; Selke, M. Photochem. Photobiol. 2014, 90, 257–274.

(22) (a) Abdel-Shafi, A. A.; Worrall, D. R.; Ershov, A. Y. Dalton Trans. 2004, 1, 30–36. (b) Abdel-Shafi, A. A.; Bourdelande, J. L.; Ali, S. S. Dalton Trans. 2007, 24, 2510–2516.

(23) Foxon, S. P.; Alamiry, M. A. H.; Walker, M. G.; Meijer, A. J. H. M.; Sazanovich, I. V.; Weinstein, J. A.; Thomas, J. A. J. Phys. Chem. A 2009, 113, 12754–12762.

(24) Sun, Y.; Joyce, L.; Dickson, N. M.; Turro, C. Chem. Commun. 2010, 46, 2426.

(25) (a) Friedman, A. E.; Chambron, J. C.; Sauvage, J. P.; Turro, N. J.; Barton, J. K. J. Am. Chem. Soc. 1990, 112, 4960. (b) Jenkins, Y.; Barton, J. K. J. Am. Chem. Soc. 1992, 114, 8736. (c) Hartshorn, R. M.; Barton, J. K. J. Am. Chem. Soc. 1992, 114, 8736. (d) Jenkins, Y.; Friedman, A. E.; Turro, N. J.; Barton, J. K. Biochemistry 1992, 31, 10809. (e) Homlin, R. E.; Barton, J. K. Inorg. Chem. 1995, 37, 29.

(26) (a) Olofsson, J.; Oenfelt, B.; Lincoln, P. J. Phys. Chem. A 2004, 108, 4391. (b) Olofsson, J.; Wilhelmsson, L. M.; Lincoln, P. J. Am. Chem. Soc. 2004, 126, 15458. (c) Westerlund, F.; Eng, M. P.; Winters, M. U.; Lincoln, P. J. Phys. Chem. B 2007, 111, 310.

(27) Nair, R. B.; Murphy, C. J. J. Inorg. Biochem. 1998, 69, 129.

(28) Liu, Y.; Turner, D. B.; Singh, T. N.; Angeles-Boza, A. M.; Chouai, A.; Dunbar, K. R.; Turro, C. J. Am. Chem. Soc. 2009, 131, 26–27.

(29) Lutterman, D. A.; Fu, P. K.; Turro, C. J. Am. Chem. Soc. 2006, 128, 738.

(30) Singh, T. N.; Turro, C. Inorg. Chem. 2004, 43, 7260.

(31) Wachter, E.; Heidary, D. K.; Howerton, B. S.; Parkin, S.; Glazer, E. C. Chem. Commun. 2012, 48, 9649–9451.

(32) (a) Ford, P. C. Coord. Chem. Rev. 1970, 5, 75–99. (b) Ford, P. C. Coord. Chem. Rev. 1982, 44, 61–82. (c) Ford, P. C.; Wink, D.; Dibenedetto, J. Prog. Inorg. Chem. 1983, 30, 213–271.

(33) Tfouni, E. Coord. Chem. Rev. 2000, 196, 281–305.

(34) Foxon, S. P.; Alamiry, M. A. H.; Walker, M. G.; Meijer, A. J. H. M.; Sazanovich, I. V.; Weinstein, J. A.; Thomas, J. A. J. Phys. Chem. A 2009, 113, 12754–12762.

(35) Freedman, D. A.; Evju, J. K.; Pomije, M. K.; Mann, K. R. Inorg. Chem. 2001, 40, 5711–5715.

(36) Toyama, M.; Inoue, K.; Iwamatsu, S.; Nagao, N. Bull. Chem. Soc. Jpn. 2006, 79, 1525–1534.

(37) Foxon, S. P.; Green, C.; Walker, M. G.; Wragg, A.; Adams, H.; Weinstein, J. A.; Parker, S. C.; Meijer, A. J. H. M.; Thomas, J. A. Inorg. Chem. 2012, 51, 463–471.

(38) Liu, Y.; Hammitt, R.; Thummel, R. P.; Turro, C. J. Phys. Chem. B 2010, 46, 2426–2428.

(39) Burdzinski, G.; Hackett, J. C.; Wang, J.; Gustafson, T. L.; Hadad, C. M.; Platz, M. S. J. Am. Chem. Soc. 2006, 128, 13402–13411.

(40) Nakayama, T.; Amijima, Y.; Ibuki, K.; Hamanoue, K. Rev. Sci. Instrum. 1997, 68, 4364–4371.

(41) Bhattacharyya, K.; Das, P. K. Chem. Phys. Lett. 1985, 116, 326.

(42) Monalti, M.; Credi, A.; Prodi, L.; Gandolfi, M. T. Handbook of Photochemistry, 3rd ed.; Taylor & Francis Group: Boca Raton, FL, 2006; pp 601–616.

(43) Peña, B.; David, A.; Pavani, C.; Baptista, M. S.; Pellis, J.-P.; Turro, C.; Dunbar, K. R. Organometallics 2014, 33, 1100–1103.

(44) Peña, B.; Leed, N. A.; Dunbar, K. R.; Turro, C. J. Phys. Chem. C 2012, 116, 22186–22195.

(45) Albani, B. A.; Durr, C. B.; Turro, C. J. Phys. Chem. A 2013, 117, 13885–13892.

(46) (a) Malouf, G.; Ford, P. C. J. Am. Chem. Soc. 1974, 96, 601–603. (b) Malouf, G.; Ford, P. C. J. Am. Chem. Soc. 1977, 99, 7213–7221. (c) Durante, V. A.; Ford, P. C. Inorg. Chem. 1979, 18, 588–593.

(47) (a) Martinez, M. S. J. Photochem. Photobiol. A: Chemistry 1999, 122, 103–108. (b) Pavanin, L. A.; da Rocha, Z. N.; Giesbrecht, E.; Tfouni, E. Inorg. Chem. 1991, 30, 2185–2190.

(48) (a) Sullivan, B. P.; Salmon, D. J.; Meyer, T. J. Inorg. Chem. 1978, 17, 3334–3341. (b) Durham, B.; Walsh, J. L.; Carter, C. L.; Meyer, T. J. Inorg. Chem. 1980, 19, 860–865. (c) Caspar, J. V.; Meyer, T. J. Inorg. Chem. 1983, 22, 2444–2453.

(49) (a) Durham, B.; Caspar, J. V.; Nagle, J. K.; Meyer, T. J. J. Am. Chem. Soc. 1982, 104, 4803–4810. (b) Allen, G. H.; White, R. P.; Rillema, D. P.; Meyer, T. J. J. Am. Chem. Soc. 1984, 106, 2613–2620. (c) Rillema, D. P.; Taghdiri, D. G.; Jones, D. S.; Keller, C. D.; Worl, L. A.; Meyer, T. J.; Levy, H. Inorg. Chem. 1987, 26, 578–585.

F

dx.doi.org/10.1021/ja508272h | J. Am. Chem. Soc. XXXX, XXX, XXX–XXX

583 (50) Respondek, T.; Sharm, R.; Herroon, M. K.; Garner, R. N.;
584 Knoll, J. D.; Cueny, E.; Turro, C.; Podgorski, I.; Kodanko, J. J. *Chem.*
585 *Med. Chem.* **2014**, *9*, 1306−1315.
586 (51) Lincoln, R.; Kohler, L.; Monro, S.; Yin, H.; Stephenson, M.;
587 Zong, R.; Chouai, A.; Dorsey, C.; Hennigar, R.; Thummel, R. P.;
588 Mcfarland, S. A. *J. Am. Chem. Soc.* **2013**, *135*, 17161−17175.